NASA MEMO 4-3-59L

NASA MEMORANDUM

FORMULAS PERTINENT TO THE CALCULATION OF FLOW-FIELD EFFECTS AT SUPERSONIC SPEEDS DUE TO WING THICKNESS

By Kenneth Margolis and Miriam H. Elliott

Langley Research Center
Langley Field, Va.

NATIONAL AERONAUTICS AND SPACE ADMINISTRATION
WASHINGTON
May 1959

NATIONAL AERONAUTICS AND SPACE ADMINISTRATION

MEMORANDUM 4-3-59L

FORMULAS PERTINENT TO THE CALCULATION OF FLOW-FIELD EFFECTS AT SUPERSONIC SPEEDS DUE TO WING THICKNESS

By Kenneth Margolis and Miriam H. Elliott

SUMMARY

Expressions based on linearized supersonic-flow theory are derived for the perturbation velocity potential in space due to wing thickness for rectangular wings with biconvex airfoil sections and for arrow, delta, and quadrilateral wings with wedge-type airfoil sections. The complete range of supersonic speeds is considered subject to a minor aspect-ratio—Mach number restriction for the rectangular plan form and to the condition that the trailing edge is supersonic for the sweptback wings. The formulas presented can be utilized in determining the induced-flow characteristics at any point in the field and are readily adaptable for either numerical computation or analytical determination of any velocity components desired.

INTRODUCTION

The increasing use of auxiliary bodies such as stores and missiles on current aircraft has emphasized the need for reliable methods and procedures for predicting the load distribution, forces, and moments generated by such bodies and also the aerodynamic effects induced on these bodies by neighboring airplane components. The total loading and forces acting on stores, missiles, pylons, and so forth are required in order to design supporting structures, to predict the performance and stability characteristics of aircraft, to determine the jettison characteristics of stores, and to compute the trajectories of missiles when fired from parent aircraft.

Although considerable effort has been expended in the past in calculating the load distribution, forces, and moments acting on isolated aircraft components for the supersonic speed regime (e.g., refs. 1 to 3 and reports cited therein), somewhat less attention has been focused on the equally important problem of determining the aerodynamic effects induced by one body on neighboring airplane components. (See refs. 4

to 6 and reports mentioned therein.) The problem of determining the flow fields arising from airplane components undergoing various motions becomes a prime consideration in calculating induced aerodynamic effects. Some recent work pertaining to the calculation of flow fields at supersonic speeds may be found in references 7 to 9. In general, the available literature covers in adequate detail the flow fields arising from flat wings at an angle of attack and flat wings undergoing steady rolling or steady pitching motions.

The present paper concerns itself with the linearized-theory evaluation of the effect of wing thickness and thickness distribution on the flow fields generated by thin wings at zero angle of attack. The purpose is to present closed-form expressions for the perturbation velocity potential which in turn may be utilized to calculate by either numerical or analytical procedures the desired flow-field velocities and angularities. Wings of rectangular plan form with symmetrical biconvex profile and of delta and modified-delta plan forms with wedge-type airfoil sections are treated in detail. The complete range of supersonic speeds is considered subject to a minor aspect-ratio—Mach number restriction for the rectangular wing and to the condition that the trailing edge is supersonic for the sweptback wings.

SYMBOLS

x,y,z	rectangular coordinates of field points
$\bar{x},\bar{y},\bar{z}$	nondimensional rectangular coordinates defined as $\frac{x}{c_r}$, $\frac{y}{b/2}$, and $\frac{z}{b/2}$, respectively
z_B	z-coordinate defining airfoil section
ξ,η	rectangular coordinates of source points
V	free-stream or flight velocity
M	Mach number
β	Mach number parameter, $\sqrt{M^2 - 1}$
ϕ	perturbation velocity potential
$\phi_I,\phi_{II},\ldots\phi_{IX}$	specific evaluations of pertubation velocity potential
Λ	sweepback angle of leading edge

m	sweepback-Mach number parameter, $\beta \cot \Lambda$
δ	inclination of wing trailing edge, measured relative to root-chord extended (see fig. 2)
c_r	root chord of wing
b	wing span
S	area of wing plan form
A	wing aspect ratio, b^2/S
$\bar{A}$	aspect-ratio—Mach number parameter, $A\beta$
t	maximum thickness of local airfoil section
c	local wing chord
λ	slope of wing surface, measured in stream direction
$F_1, F_2, \ldots F_6$	functions that are given in appendix A for purposes of evaluating perturbation velocity potential for sweptback wing cases
$G_1, G_2, \ldots G_{14}$	functions that are given in appendix B for purposes of evaluating perturbation velocity potential for rectangular wing cases
$\eta_a, \eta_b, \ldots \eta_f$	specific values of variable η corresponding to various locations where Mach forecone from field point (x,y,z) intersects leading and trailing edges of wing (see fig. 3)

ANALYSIS

The analysis is based on supersonic thin-airfoil theory and on the assumptions of small disturbances and a constant velocity of sound throughout the fluid. These assumptions lead to the linearized equation for the perturbation velocity potential ϕ:

$$(1 - M^2)\phi_{xx} + \phi_{yy} + \phi_{zz} = 0 \qquad (1)$$

where M is the Mach number of the flow, and the derivatives are taken with respect to the variables x, y, and z of the rectangular coordinate system. The general expression for the linearized perturbation velocity potential in space due to a distribution of source and sink singularities in the $z = 0$ plane is (see refs. 10 and 11)

$$\phi(x,y,z) = -\frac{V}{\pi}\int_R\int \frac{\lambda(\xi,\eta)\, d\xi\, d\eta}{\sqrt{(x-\xi)^2 - \left(M^2-1\right)\left[(y-\eta)^2 + z^2\right]}} \tag{2}$$

where x, y, and z are the rectangular coordinates of the field point at which the potential is desired, and ξ and η are the rectangular coordinates (analogous to x and y) of the singularities. The function $\lambda(\xi,\eta)$ represents the particular distribution of singularities for the wing under consideration and is thus, of course, dependent upon the boundary conditions imposed. For wing-thickness distributions that are amenable to thin-airfoil-theory calculations, the source-sink distribution function is related to the particular thickness distribution involved and is given as

$$\lambda(\xi,\eta) = \left[\frac{\partial}{\partial\xi} z_B(\xi,\eta)\right]_{z_B=0} \tag{3}$$

The integration indicated in equation (2) is performed over the region R that is enclosed by the traces in the $z = 0$ plane of the Mach forecone emanating from the point (x,y,z) and by the wing plan-form boundaries. (See fig. 1.) For purposes of convenience, the Mach number parameter $\beta = \sqrt{M^2 - 1}$ rather than M itself will be used in the expressions to be developed; equation (2) may then be rewritten in the more familiar form

$$\phi(x,y,z) = -\frac{V}{\pi}\int_R\int \frac{\lambda(\xi,\eta)\, d\xi\, d\eta}{\sqrt{(x-\xi)^2 - \beta^2(y-\eta)^2 - \beta^2 z^2}} \tag{4}$$

In order to obtain closed-form expressions for the potential function $\phi(x,y,z)$, it is necessary to define the slope function $\lambda(\xi,\eta)$ for the particular wing under consideration (see eq. (3)) and then to integrate over the appropriate region R. The present paper considers

delta and modified-delta wings with wedge airfoil sections and rectangular wings with symmetrical biconvex airfoil sections. (See fig. 2.) For the sweptback wings, the equation for the upper surface is given by

$$z = \frac{t}{2c} x \tag{5}$$

where x is measured positive rearward from the y-axis. (See fig. 3.) The slope function $\lambda(\xi,\eta)$ is, of course, constant for the sweptback wings and is given by

$$\lambda = \frac{t}{2c} \tag{6}$$

For the rectangular wings, the equation for the upper surface may readily be derived as

$$z = 2t \frac{x}{c}\left(1 - \frac{x}{c}\right) \tag{7}$$

where x is measured positive rearward from the leading edge. The slope function $\lambda(\xi,\eta)$, which for the rectangular wings is independent of η, is found to be

$$\lambda(\xi) = \frac{4t}{c^2}\left(\frac{c}{2} - \xi\right) \tag{8}$$

In order to determine the appropriate regions of integration, the sweptback wings have been subdivided into nine cases (see fig. 4), each case being characterized by distinct Mach trace—plan-form-boundary intersections. In an analogous manner, the rectangular wings have been subdivided into eight cases (see fig. 5). Thus, if the perturbation velocity potential is desired at an arbitrary point (x,y,z), the Mach trace must be determined and then the appropriate integration performed in accordance with equation (4). The sketches given in figures 4 and 5 cover all possible cases that are required to determine completely the potential function for the wings under consideration. Note that the only restriction applicable to the sweptback wings is that the trailing edge is supersonic; for the rectangular wings, the side edges may not interact (expressed mathematically by the condition $A\beta \geqq 1$). (See fig. 2.) It is of interest to point out that cases VII, VIII, and IX for the sweptback wings can occur only when the wing has a supersonic leading edge.

In order to define mathematically the required regions of integration, the η coordinate of the point of intersection between the Mach forecone $\xi = x - \beta\sqrt{(y - \eta)^2 + z^2}$ and each plan-form boundary must be obtained. The specific intersection points are indicated by the filled-in circles shown in figure 3, and the associated η values are readily found by simple algebraic processes to be

$$\eta_a = \frac{\cot \Lambda}{1 - \beta^2\cot^2\Lambda}\left[-x - \beta^2 y \cot \Lambda + \beta\sqrt{(x \cot \Lambda + y)^2 + z^2(1 - \beta^2\cot^2\Lambda)}\right] \tag{9}$$

$$\eta_b = \frac{\cot \Lambda}{1 - \beta^2\cot^2\Lambda}\left[x - \beta^2 y \cot \Lambda - \beta\sqrt{(x \cot \Lambda - y)^2 + z^2(1 - \beta^2\cot^2\Lambda)}\right] \tag{10}$$

$$\eta_c = \frac{\tan \delta}{\beta^2\tan^2\delta - 1}\left[x - c_r + \beta^2 y \tan \delta - \beta\sqrt{\left[(x - c_r)\tan \delta + y\right]^2 + z^2(1 - \beta^2\tan^2\delta)}\right] \tag{11}$$

$$\eta_d = \frac{\tan \delta}{\beta^2\tan^2\delta - 1}\left[c_r - x + \beta^2 y \tan \delta + \beta\sqrt{\left[(x - c_r)\tan \delta - y\right]^2 + z^2(1 - \beta^2\tan^2\delta)}\right] \tag{12}$$

$$\eta_e = \frac{\tan \delta}{\beta^2\tan^2\delta - 1}\left[c_r - x + \beta^2 y \tan \delta - \beta\sqrt{\left[(x - c_r)\tan \delta - y\right]^2 + z^2(1 - \beta^2\tan^2\delta)}\right] \tag{13}$$

$$\eta_f = \frac{\cot \Lambda}{1 - \beta^2\cot^2\Lambda}\left[x - \beta^2 y \cot \Lambda + \beta\sqrt{(x \cot \Lambda - y)^2 + z^2(1 - \beta^2\cot^2\Lambda)}\right] \tag{14}$$

For the rectangular wing ($\Lambda = 0^\circ$ and $\delta = 90^\circ$), η_e and η_f are the same as η_c and η_a, respectively, and considerable simplification results in equations (9) to (12). The simplified expressions for η_a to η_d are as follows:

$$\eta_a = \frac{\beta y - \sqrt{x^2 - \beta^2 z^2}}{\beta} \tag{15}$$

$$\eta_b = \frac{\beta y + \sqrt{x^2 - \beta^2 z^2}}{\beta} \tag{16}$$

$$\eta_c = \frac{\beta y - \sqrt{(x - c)^2 - \beta^2 z^2}}{\beta} \tag{17}$$

$$\eta_d = \frac{\beta y + \sqrt{(x - c)^2 - \beta^2 z^2}}{\beta} \tag{18}$$

The integral expressions for the perturbation velocity potential corresponding to the nine cases for the sweptback wing (see fig. 4) and the eight cases for the rectangular wing (see fig. 5) may now be explicitly determined. For purposes of convenience appendixes A and B present for the sweptback wings and rectangular wings, respectively, the various conditions associated with each potential function as well as the specific formulas (F and G functions) required to define the potential.

The following equations result for the nine sweptback-wing cases, where the slope λ is constant and defined by equation (6):

Case I:

$$-\frac{\pi}{V\lambda}\frac{\phi_I(x,y,z)}{b/2} = F_1 \tag{19}$$

Case II:

$$-\frac{\pi}{V\lambda}\frac{\phi_{II}(x,y,z)}{b/2} = F_1 + F_2 \tag{20}$$

Case III:

$$-\frac{\pi}{V\lambda}\frac{\phi_{III}(x,y,z)}{b/2} = F_1 + F_2 + F_3 \tag{21}$$

Case IV:

$$-\frac{\pi}{V\lambda}\frac{\phi_{IV}(x,y,z)}{b/2} = F_1 + F_3 - F_5 \tag{22}$$

Case V:

$$-\frac{\pi}{V\lambda}\frac{\phi_V(x,y,z)}{b/2} = F_1 - F_5 \tag{23}$$

Case VI:

$$-\frac{\pi}{V\lambda}\frac{\phi_{VI}(x,y,z)}{b/2} = F_1 + F_2 + F_3 + F_4 \tag{24}$$

Case VII:

$$-\frac{\pi}{V\lambda}\frac{\phi_{VII}(x,y,z)}{b/2} = F_3 - F_5 + F_6 \tag{25}$$

Case VIII:

$$-\frac{\pi}{V\lambda}\frac{\phi_{VIII}(x,y,z)}{b/2} = F_6 - F_5 \tag{26}$$

Case IX:

$$-\frac{\pi}{V\lambda}\frac{\phi_{IX}(x,y,z)}{b/2} = F_6 \tag{27}$$

For the eight rectangular-wing cases, the following formulas result:

Case I:

$$-\frac{\pi}{2V\left(\frac{t}{c}\right)}\frac{\phi_I(x,y,z)}{b/2} = 2G_4 + G_5 \tag{28}$$

Case II:

$$\left.\begin{aligned} \text{For } y \leq \frac{b}{2}, \quad -\frac{\pi}{2V\left(\frac{t}{c}\right)}\frac{\phi_{II}(x,y,z)}{b/2} &= G_1 - G_3 + G_4 + G_5 \\ \text{For } y > \frac{b}{2}, \quad -\frac{\pi}{2V\left(\frac{t}{c}\right)}\frac{\phi_{II}(x,y,z)}{b/2} &= G_2 - G_3 + G_4 \end{aligned}\right\} \tag{29}$$

Case III:

$$-\frac{\pi}{2V\left(\frac{t}{c}\right)}\frac{\phi_{III}(x,y,z)}{b/2} = G_1 + G_{10} - G_3 + G_{11} + G_5 \tag{30}$$

Case IV:

$$-\frac{\pi}{2V\left(\frac{t}{c}\right)}\frac{\phi_{IV}(x,y,z)}{b/2}=0 \tag{31}$$

Case V:

$$-\frac{\pi}{2V\left(\frac{t}{c}\right)}\frac{\phi_{V}(x,y,z)}{b/2}=G_1+G_{10}-G_3+G_{11}+G_5-G_6-G_{12}+G_8-G_{13}-G_{14} \tag{32}$$

Case VI:

$$-\frac{\pi}{2V\left(\frac{t}{c}\right)}\frac{\phi_{VI}(x,y,z)}{b/2}=G_1+G_{10}-G_3+G_{11}-2G_4 \tag{33}$$

Case VII:

$$\left.\begin{aligned}&\text{For}\quad y\leq\frac{b}{2},\quad -\frac{\pi}{2V\left(\frac{t}{c}\right)}\frac{\phi_{VII}(x,y,z)}{b/2}=G_1-G_6-G_3+G_8+G_9\\&\text{For}\quad y>\frac{b}{2},\quad -\frac{\pi}{2V\left(\frac{t}{c}\right)}\frac{\phi_{VII}(x,y,z)}{b/2}=G_2-G_7-G_3+G_8-G_9\end{aligned}\right\} \tag{34}$$

Case VIII:

$$-\frac{\pi}{2V\left(\frac{t}{c}\right)}\frac{\phi_{VIII}(x,y,z)}{b/2}=G_1-G_3-G_4 \tag{35}$$

DISCUSSION

The formulas presented in the previous section enable the direct evaluation of the perturbation velocity potential in the vicinity of rectangular wings with symmetrical biconvex airfoil sections and the corresponding perturbation velocity potential for delta and modified-delta wings with wedge airfoil sections. For the sweptback-wing cases with airfoil sections of arbitrary thickness distribution, the well-known superposition procedure can be employed by using the given formulas with appropriate values for the parameters substituted therein. A graphical presentation of the mechanics involved in superposing the basic solution is given in figure 6. Note that each component part may be

directly evaluated from the expressions presented in equations (6) and (19) to (27) and those given in appendix A.

In connection with the formulas applicable for the sweptback wings, it should be pointed out that for the special conditions of $\beta \cot \Lambda = 1$ (sonic leading edge) and $\beta \tan \delta = \infty$ (unswept trailing edge) the functions of appendix A are simplified to considerable extent by conventional procedures. The following relationships should be used in the event certain terms (for convenience denoted by N) take on imaginary values:

For $|N| < 1$,

$$\left.\begin{aligned} \cosh^{-1} N &= i \cos^{-1} N \\ \cos^{-1} N &= -i \cosh^{-1} N \end{aligned}\right\} \tag{36}$$

and, for $|N| > 1$,

$$\left.\begin{aligned} \cosh^{-1} N &= -i \cos^{-1} N \\ \cos^{-1} N &= i \cosh^{-1} N \end{aligned}\right\} \tag{37}$$

Care should be exercised in extracting only positive roots from radical terms. To minimize the possibility of errors in the final formulas, all derivations have been checked analytically by independent means and also checked numerically by graphical integration procedures.

The formulas presented for the perturbation velocity potential may be differentiated by either numerical or analytical procedures to obtain the various velocity components which in turn will enable the direct evaluation of flow-field effects on neighboring airplane or missile components. An approach that has proved to be very efficient consists of computing the potential function and its variation along a given direction and then measuring the slopes either graphically or numerically to obtain the desired velocity component.

CONCLUDING REMARKS

Expressions based on linearized supersonic-flow theory are derived for the perturbation velocity potential in space due to wing thickness for rectangular wings with biconvex airfoil sections and for arrowhead, delta, and quadrilateral wings with wedge-type airfoil sections. The complete range of supersonic speed is considered subject to a minor

aspect-ratio—Mach number restriction for the rectangular plan form and to the condition that the trailing edge is supersonic for the sweptback wings. The formulas presented can be utilized in determining the induced-flow characteristics at any point in the field and are readily adaptable for either numerical computation or analytical determination of any velocity components desired.

Langley Research Center,
National Aeronautics and Space Administration,
Langley Field, Va., December 24, 1958.

APPENDIX A

MATHEMATICAL CONDITIONS AND FUNCTIONS PERTINENT TO EVALUATION OF VELOCITY POTENTIAL FOR SWEPTBACK-WING CASES

In order to determine the specific sweptback-wing case applicable for a given point (x,y,z), the following mathematical conditions may be utilized:

Case I:

$$\eta_a < 0 < \eta_b$$

η_c and η_d are imaginary

Case II:

$$-\frac{b}{2} < \eta_c < 0$$

$$\eta_d < \frac{b}{2}$$

Case III:

$$-\frac{b}{2} < \eta_c < 0$$

$$\eta_d > \frac{b}{2}$$

Case IV:

$$0 < \eta_e < \frac{b}{2} < \eta_d$$

Case V:

$$0 < \eta_e < \eta_d < \frac{b}{2}$$

Case VI:

$$\eta_a < -\frac{b}{2}$$

$$\eta_b > \frac{b}{2}$$

Case VII:

$$0 < \eta_f < \eta_e < \frac{b}{2} < \eta_d$$

Case VIII:

$$0 < \eta_f < \eta_e < \eta_d < \frac{b}{2}$$

Case IX:

$$0 < \eta_f < \eta_b < \frac{b}{2}$$

η_e and η_d are imaginary

The various η functions referred to in the preceding conditions are defined by equations (9) to (14) in the text.

The formulas for the perturbation velocity potential ϕ are presented for the various cases in equations (19) to (27) in the text. The functions F_1 to F_6 are used therein for purposes of simplification and are defined as follows in terms of the nondimensional space coordinates $\bar{x}$, $\bar{y}$, and $\bar{z}$ and the plan-form—Mach number parameters $\bar{A}$ and m (where $\bar{A} = A\beta$ and $m = \beta \cot \Lambda$):

$$F_1 = \frac{4m\bar{x} - \bar{A}\bar{y}}{\bar{A}\sqrt{1 - m^2}} \cosh^{-1} \frac{4\bar{x} + \bar{A}m\bar{y}}{\sqrt{(4m\bar{x} + \bar{A}\bar{y})^2 + \bar{A}^2\bar{z}^2(1 - m^2)}} - \bar{z} \tan^{-1} \frac{m\bar{z}\sqrt{16\bar{x}^2 - \bar{A}^2(\bar{y}^2 + \bar{z}^2)}}{\bar{A}(\bar{y}^2 + \bar{z}^2) + 4m\bar{x}\bar{y}} +$$

$$\frac{4m\bar{x} - \bar{A}\bar{y}}{\bar{A}\sqrt{1 - m^2}} \cosh^{-1} \frac{4\bar{x} - \bar{A}m\bar{y}}{\sqrt{(4m\bar{x} - \bar{A}\bar{y})^2 + \bar{A}^2\bar{z}^2(1 - m^2)}} - \bar{z} \tan^{-1} \frac{m\bar{z}\sqrt{16\bar{x}^2 - \bar{A}^2(\bar{y}^2 + \bar{z}^2)}}{\bar{A}(\bar{y}^2 + \bar{z}^2) - 4m\bar{x}\bar{y}} \qquad \text{(A1)}$$

$$F_2 = -\frac{4m(\bar{x}-1)+\bar{y}(\bar{A}-4m)}{\sqrt{m^2\left(\bar{A}^2-16\right)+8\bar{A}m-\bar{A}^2}}\cos^{-1}\frac{4(\bar{x}-1)(\bar{A}-4m)+\bar{A}^2m\bar{y}}{\bar{A}\sqrt{\left[4m(\bar{x}-1)+\bar{y}(\bar{A}-4m)\right]^2-\bar{z}^2\left[m^2\left(\bar{A}^2-16\right)+8\bar{A}m-\bar{A}^2\right]}}+$$

$$\bar{z}\tan^{-1}\frac{m\bar{z}\sqrt{16(\bar{x}-1)^2-\bar{A}^2\left(\bar{y}^2+\bar{z}^2\right)}}{(\bar{A}-4m)\left(\bar{y}^2+\bar{z}^2\right)+4m\bar{y}(\bar{x}-1)}+\bar{z}\tan^{-1}\frac{m\bar{z}\sqrt{16(\bar{x}-1)^2-\bar{A}^2\left(\bar{y}^2+\bar{z}^2\right)}}{(\bar{A}-4m)\left(\bar{y}^2+\bar{z}^2\right)-4m\bar{y}(\bar{x}-1)}-$$

$$\frac{4m(\bar{x}-1)-\bar{y}(\bar{A}-4m)}{\sqrt{m^2\left(\bar{A}^2-16\right)+8\bar{A}m-\bar{A}^2}}\cos^{-1}\frac{4(\bar{x}-1)(\bar{A}-4m)-\bar{A}^2m\bar{y}}{\bar{A}\sqrt{\left[4m(\bar{x}-1)-\bar{y}(\bar{A}-4m)\right]^2-\bar{z}^2\left[m^2\left(\bar{A}^2-16\right)+8\bar{A}m-\bar{A}^2\right]}} \tag{A2}$$

$$F_3 = -\frac{4m\bar{x}-\bar{A}\bar{y}}{\bar{A}\sqrt{1-m^2}}\cosh^{-1}\frac{4m\bar{x}-\bar{A}+\bar{A}m^2(1-\bar{y})}{m\sqrt{(4m\bar{x}-\bar{A}\bar{y})^2+\bar{A}^2\bar{z}^2(1-m^2)}}+\bar{z}\tan^{-1}\frac{\bar{z}\sqrt{(4m\bar{x}-\bar{A})^2-\bar{A}^2m^2\left[(1-\bar{y})^2+\bar{z}^2\right]}}{\bar{A}\left[\bar{z}^2-\bar{y}(1-\bar{y})\right]+4m\bar{x}(1-\bar{y})}+$$

$$\frac{4m(\bar{x}-1)-\bar{y}(\bar{A}-4m)}{\sqrt{m^2\left(\bar{A}^2-16\right)+8\bar{A}m-\bar{A}^2}}\cos^{-1}\frac{(\bar{A}-4m)(4m\bar{x}-\bar{A})+\bar{A}^2m^2(1-\bar{y})}{\bar{A}m\sqrt{\left[4m(\bar{x}-1)-\bar{y}(\bar{A}-4m)\right]^2-\bar{z}^2\left[m^2\left(\bar{A}^2-16\right)+8\bar{A}m-\bar{A}^2\right]}}-$$

$$\bar{z}\tan^{-1}\frac{\bar{z}\sqrt{(4m\bar{x}-\bar{A})^2-\bar{A}^2m^2\left[(1-\bar{y})^2+\bar{z}^2\right]}}{(\bar{A}-4m)\left[\bar{z}^2-\bar{y}(1-\bar{y})\right]+4m(\bar{x}-1)(1-\bar{y})} \tag{A3}$$

$$F_4 = \frac{4m(\bar{x}-1)+\bar{y}(\bar{A}-4m)}{\sqrt{m^2\left(\bar{A}^2-16\right)+8\bar{A}m-\bar{A}^2}}\cos^{-1}\frac{(\bar{A}-4m)(4m\bar{x}-\bar{A})+\bar{A}^2m^2(1+\bar{y})}{\bar{A}m\sqrt{\left[4m(\bar{x}-1)+\bar{y}(\bar{A}-4m)\right]^2-\bar{z}^2\left[m^2\left(\bar{A}^2-16\right)+8\bar{A}m-\bar{A}^2\right]}}-$$

$$\bar{z}\tan^{-1}\frac{\bar{z}\sqrt{(4m\bar{x}-\bar{A})^2-\bar{A}^2\left[m^2(1+\bar{y})^2+\bar{z}^2\right]}}{(\bar{A}-4m)\left[\bar{z}^2+\bar{y}(1+\bar{y})\right]+4m(\bar{x}-1)(1+\bar{y})}-\frac{4m\bar{x}+\bar{A}\bar{y}}{\bar{A}\sqrt{1-m^2}}\cosh^{-1}\frac{4m\bar{x}-\bar{A}+\bar{A}m^2(1+\bar{y})}{m\sqrt{(4m\bar{x}+\bar{A}\bar{y})^2+\bar{A}^2\bar{z}^2(1-m^2)}}+$$

$$\bar{z}\tan^{-1}\frac{\bar{z}\sqrt{(4m\bar{x}-\bar{A})^2-\bar{A}^2m^2\left[(1+\bar{y})^2+\bar{z}^2\right]}}{\bar{A}\left[\bar{z}^2+\bar{y}(1+\bar{y})\right]+4m\bar{x}(1+\bar{y})} \tag{A4}$$

$$F_5 = \left|\frac{4m(\bar{x}-1)-\bar{y}(\bar{A}-4m)}{\sqrt{m^2\left(\bar{A}^2-16\right)+8\bar{A}m-\bar{A}^2}}-\bar{z}\right|\pi \tag{A5}$$

$$F_6 = \left(\frac{4m\bar{x}-\bar{A}\bar{y}}{\bar{A}\sqrt{m^2-1}}-\bar{z}\right)\pi \tag{A6}$$

APPENDIX B

MATHEMATICAL CONDITIONS AND FUNCTIONS PERTINENT TO EVALUATION OF VELOCITY POTENTIAL FOR RECTANGULAR-WING CASES

In order to determine the specific rectangular-wing case applicable for a given point (x,y,z), the following mathematical conditions may be utilized:

Case I:

$$x < c + \beta z$$

$$-\frac{b}{2} < \eta_a < \eta_b < \frac{b}{2}$$

Case II:

$$\text{For } x < c + \beta z, \quad -\frac{b}{2} < \eta_a < \frac{b}{2} < \eta_b$$

$$\text{For } x > c + \beta z, \quad -\frac{b}{2} < \eta_a < \frac{b}{2} < \eta_c$$

Case III:

$$\text{For } x < c + \beta z, \quad \eta_a < -\frac{b}{2}, \quad \eta_b > \frac{b}{2}$$

$$\text{For } x > c + \beta z, \quad \eta_a < -\frac{b}{2}, \quad \eta_c > \frac{b}{2}$$

Case IV:

$$x > c + \beta z$$

$$-\frac{b}{2} < \eta_a < \eta_b < \frac{b}{2}$$

Case V:

$$\eta_c < -\frac{b}{2}$$

$$\eta_d > \frac{b}{2}$$

Case VI:

$$\eta_a < -\frac{b}{2} < \eta_c < \eta_d < \frac{b}{2} < \eta_b$$

Case VII:

$$-\frac{b}{2} < \eta_a < \eta_c < \frac{b}{2} < \eta_d$$

Case VIII:

$$-\frac{b}{2} < \eta_a < \eta_c < \eta_d < \frac{b}{2} < \eta_b$$

The various η functions referred to in the preceding conditions are defined by equations (15) to (18) in the text.

The formulas for the perturbation velocity potential ϕ are presented for the various cases in equations (28) to (35) in the text. The functions G_1 to G_{14} are used therein for purposes of simplification and are defined as follows in terms of the nondimensional space coordinates $\bar{x}$, $\bar{y}$, and $\bar{z}$ and the aspect-ratio—Mach number parameter $\overline{A}$ (where $\overline{A} = A\beta$):

$$G_1 = (1 - 2\bar{x})\left\{(1 - \bar{y})\cosh^{-1}\frac{2\bar{x}}{\overline{A}\sqrt{(\bar{y} - 1)^2 + \bar{z}^2}} - \right.$$

$$\frac{\bar{z}}{2}\cos^{-1}\frac{\bar{z}^2\left(4\bar{x}^2 - \overline{A}^2\bar{z}^2\right) - (\bar{y} - 1)^2\left(4\bar{x}^2 + \overline{A}^2\bar{z}^2\right)}{\left(4\bar{x}^2 - \overline{A}^2\bar{z}^2\right)\left[(\bar{y} - 1)^2 + \bar{z}^2\right]} -$$

$$\left.\frac{\bar{x}}{\overline{A}}\cos^{-1}\frac{2\overline{A}^2(\bar{y} - 1)^2 - 4\bar{x}^2 + \overline{A}^2\bar{z}^2}{4\bar{x}^2 - \overline{A}^2\bar{z}^2}\right\} \qquad (B1)$$

$$G_2 = (1 - 2\bar{x}) \left\{ (1 - \bar{y}) \cosh^{-1} \frac{2\bar{x}}{\bar{A}\sqrt{(\bar{y} - 1)^2 + \bar{z}^2}} + \right.$$

$$\frac{\bar{z}}{2} \cos^{-1} \frac{\bar{z}^2\left(4\bar{x}^2 - \bar{A}^2\bar{z}^2\right) - (\bar{y} - 1)^2\left(4\bar{x}^2 + \bar{A}^2\bar{z}^2\right)}{\left(4\bar{x}^2 - \bar{A}^2\bar{z}^2\right)\left[(\bar{y} - 1)^2 + \bar{z}^2\right]} +$$

$$\left. \frac{\bar{x}}{\bar{A}} \cos^{-1} \frac{2\bar{A}^2(\bar{y} - 1)^2 - 4\bar{x}^2 + \bar{A}^2\bar{z}^2}{4\bar{x}^2 - \bar{A}^2\bar{z}^2} \right\} \tag{B2}$$

$$G_3 = \frac{\bar{y} - 1}{2}\sqrt{4\bar{x}^2 - \bar{A}^2\left[(\bar{y} - 1)^2 + \bar{z}^2\right]} + \frac{4\bar{x}^2 - \bar{A}^2\bar{z}^2}{2\bar{A}} \sin^{-1} \frac{\bar{A}(\bar{y} - 1)}{\sqrt{4\bar{x}^2 - \bar{A}^2\bar{z}^2}} \tag{B3}$$

$$G_4 = \left[\frac{4\bar{x}^2 - \bar{A}^2\bar{z}^2}{2\bar{A}} - (1 - 2\bar{x})\bar{z}\right]\frac{\pi}{2} \tag{B4}$$

$$G_5 = (1 - 2\bar{x})\frac{2\pi\bar{x}}{\bar{A}} \tag{B5}$$

$$G_6 = (1 - 2\bar{x}) \left\{ (1 - \bar{y}) \cosh^{-1} \frac{2(\bar{x} - 1)}{\bar{A}\sqrt{(\bar{y} - 1)^2 + \bar{z}^2}} - \right.$$

$$\frac{\bar{z}}{2} \cos^{-1} \frac{\bar{z}^2\left[4(\bar{x} - 1)^2 - \bar{A}^2\bar{z}^2\right] - (\bar{y} - 1)^2\left[4(\bar{x} - 1)^2 + \bar{A}^2\bar{z}^2\right]}{\left[4(\bar{x} - 1)^2 - \bar{A}^2\bar{z}^2\right]\left[(\bar{y} - 1)^2 + \bar{z}^2\right]} -$$

$$\left. \frac{\bar{x} - 1}{\bar{A}} \cos^{-1} \frac{2\bar{A}^2(\bar{y} - 1)^2 - 4(\bar{x} - 1)^2 + \bar{A}^2\bar{z}^2}{4(\bar{x} - 1)^2 - \bar{A}^2\bar{z}^2} \right\} \tag{B6}$$

$$G_7 = (1 - 2\bar{x})\left\{(1 - \bar{y})\cosh^{-1}\frac{2(\bar{x} - 1)}{\bar{A}\sqrt{(\bar{y} - 1)^2 + \bar{z}^2}} + \right.$$

$$\frac{\bar{z}}{2}\cos^{-1}\frac{\bar{z}^2\left[4(\bar{x} - 1)^2 - \bar{A}^2\bar{z}^2\right] - (\bar{y} - 1)^2\left[4(\bar{x} - 1)^2 + \bar{A}^2\bar{z}^2\right]}{\left[4(\bar{x} - 1)^2 - \bar{A}^2\bar{z}^2\right]\left[(\bar{y} - 1)^2 + \bar{z}^2\right]} +$$

$$\left.\frac{\bar{x} - 1}{\bar{A}}\cos^{-1}\frac{2\bar{A}^2(\bar{y} - 1)^2 - 4(\bar{x} - 1)^2 + \bar{A}^2\bar{z}^2}{4(\bar{x} - 1)^2 - \bar{A}^2\bar{z}^2}\right\} \tag{B7}$$

$$G_8 = \frac{\bar{y} - 1}{2}\sqrt{4(\bar{x} - 1)^2 - \bar{A}^2\left[(\bar{y} - 1)^2 + \bar{z}^2\right]} +$$

$$\frac{4(\bar{x} - 1)^2 - \bar{A}^2\bar{z}^2}{2\bar{A}}\sin^{-1}\frac{\bar{A}(\bar{y} - 1)}{\sqrt{4(\bar{x} - 1)^2 - \bar{A}^2\bar{z}^2}} \tag{B8}$$

$$G_9 = (1 - 2\bar{x})\frac{\pi}{\bar{A}} \tag{B9}$$

$$G_{10} = (1 - 2\bar{x})\left\{(1 + \bar{y})\cosh^{-1}\frac{2\bar{x}}{\bar{A}\sqrt{(\bar{y} + 1)^2 + \bar{z}^2}} - \right.$$

$$\frac{\bar{z}}{2}\cos^{-1}\frac{\bar{z}^2\left(4\bar{x}^2 - \bar{A}^2\bar{z}^2\right) - (\bar{y} + 1)^2\left(4\bar{x}^2 + \bar{A}^2\bar{z}^2\right)}{\left(4\bar{x}^2 - \bar{A}^2\bar{z}^2\right)\left[(\bar{y} + 1)^2 + \bar{z}^2\right]} -$$

$$\left.\frac{\bar{x}}{\bar{A}}\cos^{-1}\frac{2\bar{A}^2(\bar{y} + 1)^2 - 4\bar{x}^2 + \bar{A}^2\bar{z}^2}{4\bar{x}^2 - \bar{A}^2\bar{z}^2}\right\} \tag{B10}$$

$$G_{11} = \frac{\bar{y} + 1}{2}\sqrt{4\bar{x}^2 - \overline{A}^2\left[(\bar{y} + 1)^2 + \bar{z}^2\right]} + \frac{4\bar{x}^2 - \overline{A}^2\bar{z}^2}{2\overline{A}} \sin^{-1} \frac{\overline{A}(\bar{y} + 1)}{\sqrt{4\bar{x}^2 - \overline{A}^2\bar{z}^2}} \tag{B11}$$

$$G_{12} = (1 - 2\bar{x})\left\{(1 + \bar{y})\cosh^{-1} \frac{2(\bar{x} - 1)}{\overline{A}\sqrt{(\bar{y} + 1)^2 + \bar{z}^2}} - \right.$$

$$\frac{\bar{z}}{2} \cos^{-1} \frac{\bar{z}^2\left[4(\bar{x} - 1)^2 - \overline{A}^2\bar{z}^2\right] - (\bar{y} + 1)^2\left[4(\bar{x} - 1)^2 + \overline{A}^2\bar{z}^2\right]}{\left[4(\bar{x} - 1)^2 - \overline{A}^2\bar{z}^2\right]\left[(\bar{y} + 1)^2 + \bar{z}^2\right]} -$$

$$\left. \frac{\bar{x} - 1}{\overline{A}} \cos^{-1} \frac{2\overline{A}^2(\bar{y} + 1)^2 - 4(\bar{x} - 1)^2 + \overline{A}^2\bar{z}^2}{4(\bar{x} - 1)^2 - \overline{A}^2\bar{z}^2} \right\} \tag{B12}$$

$$G_{13} = \frac{\bar{y} + 1}{2}\sqrt{4(\bar{x} - 1)^2 - \overline{A}^2\left[(\bar{y} + 1)^2 + \bar{z}^2\right]} +$$

$$\frac{4(\bar{x} - 1)^2 - \overline{A}^2\bar{z}^2}{2\overline{A}} \sin^{-1} \frac{\overline{A}(\bar{y} + 1)}{\sqrt{4(\bar{x} - 1)^2 - \overline{A}^2\bar{z}^2}} \tag{B13}$$

$$G_{14} = (1 - 2\bar{x})(\bar{x} - 1)\frac{2\pi}{\overline{A}} \tag{B14}$$

REFERENCES

1. Margolis, Kenneth, and Bobbitt, Percy J.: Theoretical Calculations of the Pressures, Forces, and Moments at Supersonic Speeds Due to Various Lateral Motions Acting on Thin Isolated Vertical Tails. NACA Rep. 1268, 1956. (Supersedes NACA TN 3373 by Margolis and NACA TN 3240 by Bobbitt.)

2. Margolis, Kenneth, Sherman, Windsor L., and Hannah, Margery E.: Theoretical Calculation of the Pressure Distribution, Span Loading, and Rolling Moment Due to Sideslip at Supersonic Speeds for Thin Sweptback Tapered Wings With Supersonic Trailing Edges and Wing Tips Parallel to the Axis of Wing Symmetry. NACA TN 2898, 1953.

3. Sacks, Alvin H.: Aerodynamic Forces, Moments, and Stability Derivatives for Slender Bodies of General Cross Section. NACA TN 3283, 1954.

4. Martin, John C., Diederich, Margaret S., and Bobbitt, Percy J.: A Theoretical Investigation of the Aerodynamics of Wing-Tail Combinations Performing Time-Dependent Motions at Supersonic Speeds. NACA TN 3072, 1954.

5. Mirels, Harold, and Haefeli, Rudolph C.: Line-Vortex Theory for Calculation of Supersonic Downwash. NACA Rep. 983, 1950.

6. Rogers, Arthur Wm.: Application of Two-Dimensional Vortex Theory to the Prediction of Flow Fields Behind Wings of Wing-Body Combinations at Subsonic and Supersonic Speeds. NACA TN 3227, 1954.

7. Bobbitt, Percy J., and Maxie, Peter J., Jr.: Sidewash in the Vicinity of Lifting Swept Wings at Supersonic Speeds. NACA TN 3938, 1957.

8. Bobbitt, Percy J.: Linearized Lifting-Surface and Lifting-Line Evaluation of Sidewash Behind Rolling Triangular Wings at Supersonic Speeds. NACA Rep. 1301, 1957. (Supersedes NACA TN 3609.)

9. Bobbitt, Percy J.: Tables for the Rapid Estimation of Downwash and Sidewash Behind Wings Performing Various Motions at Supersonic Speeds. NASA MEMO 2-20-59L, 1959.

10. Evvard, John C.: Distribution of Wave Drag and Lift in the Vicinity of Wing Tips at Supersonic Speeds. NACA TN 1382, 1947.

11. Puckett, Allen E.: Supersonic Wave Drag of Thin Airfoils. Jour. Aero. Sci., vol. 13, no. 9, Sept. 1946, pp. 475-484.

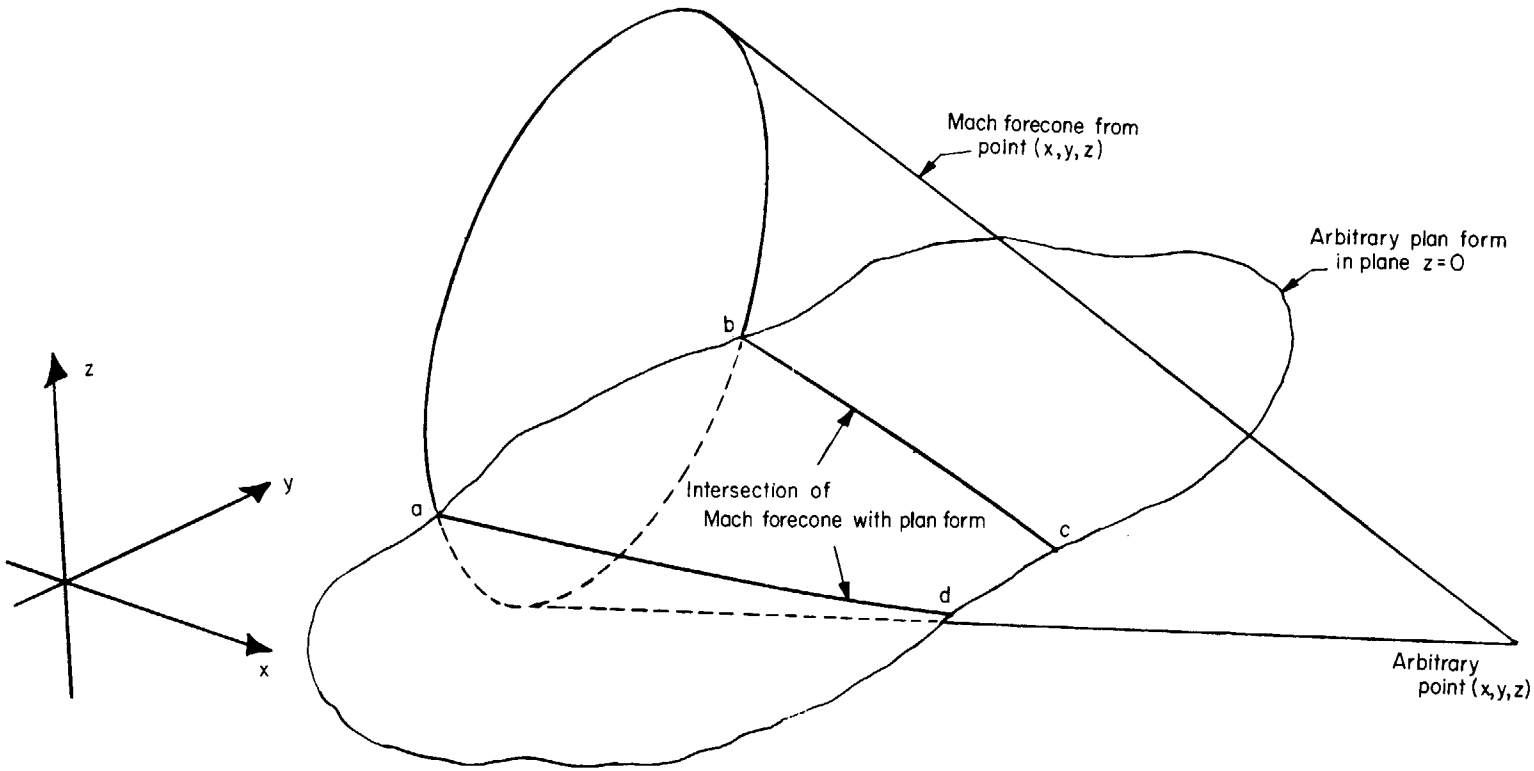

Figure 1.- Sketch illustrating Mach forecone emanating from an arbitrary point (x,y,z) in space and intersecting the wing plan form in curves ad and bc. Assume the cone to be transparent and the plan form solid; note that the region R is defined by the boundary abcd.

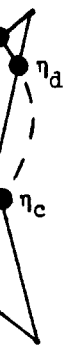

3.- Perti

22

ich the velocity
trictions on Mach
ach line emanating
te wing tip (i.e.,

24

nes of Mach forecone traces in the plane $z = 0$, indicating the plan-form
egrations required for the different sweptback-wing cases.

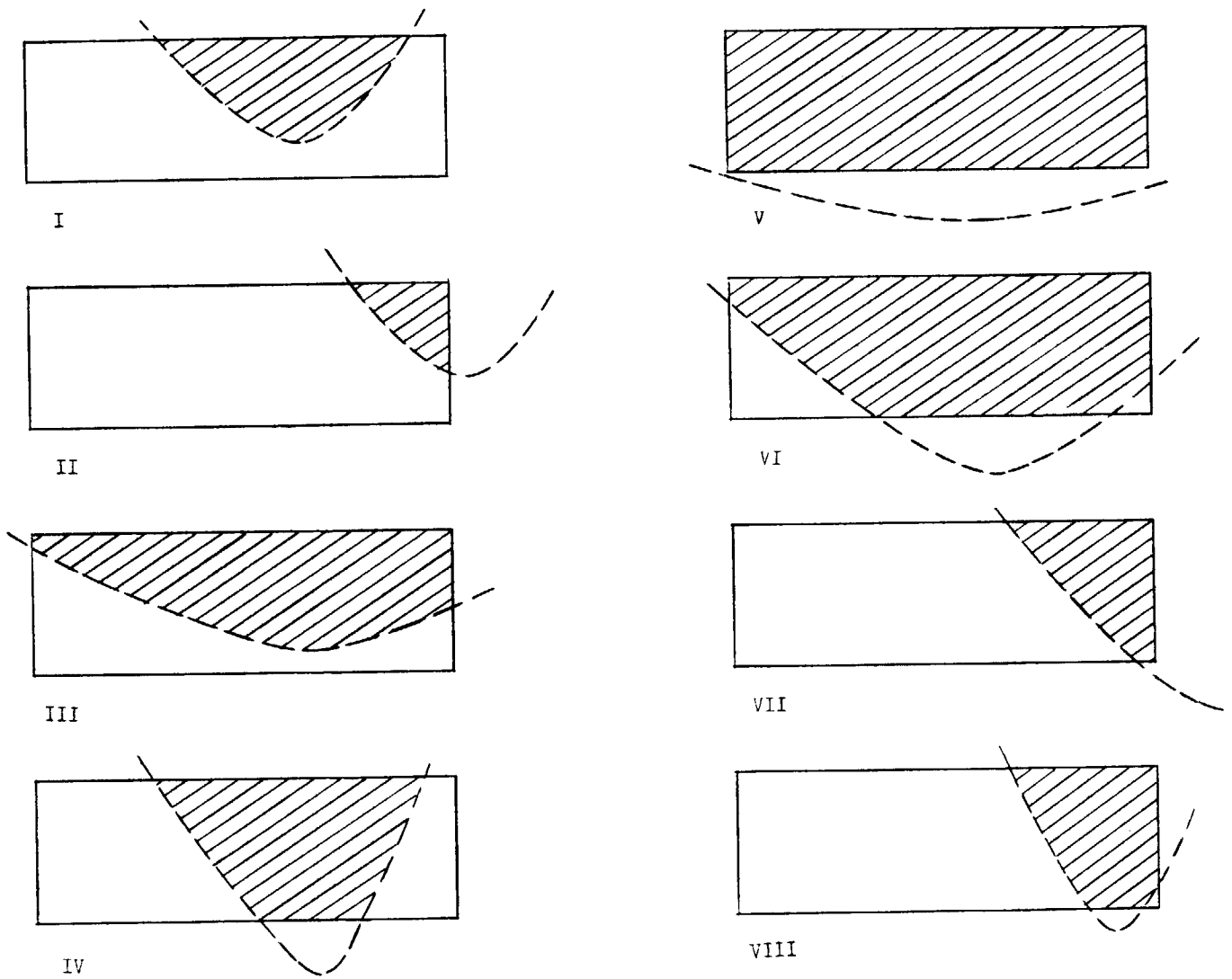

Figure 5.- Sketches of Mach forecone traces in the plane $z = 0$, indicating the plan-form integrations required for the different rectangular-wing cases.

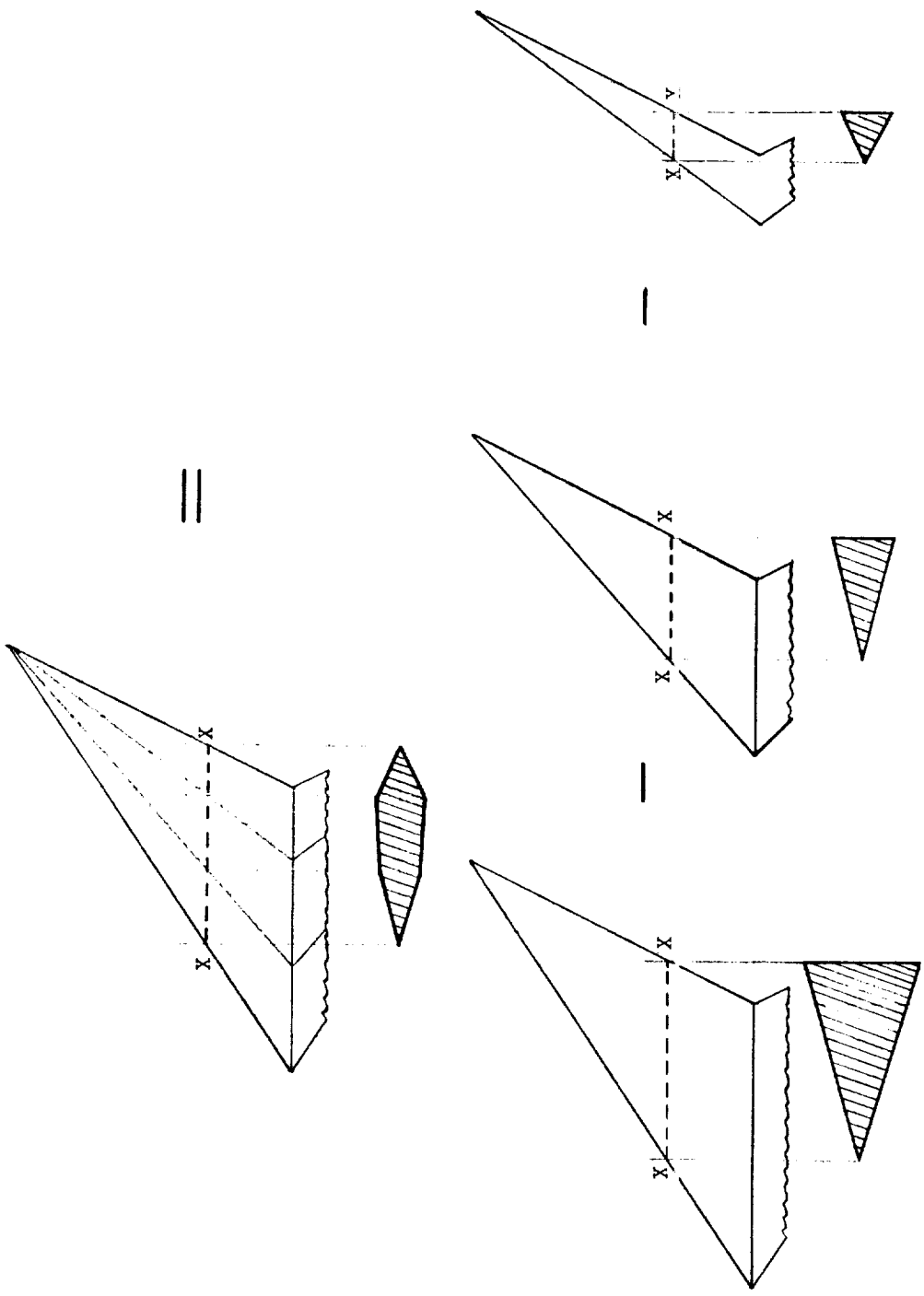

Figure 6.- Illustrative example indicating how the basic solutions for the sweptback wing with wedge thickness distribution may be superposed to obtain wings with arbitrary thickness distribution.

NASA - Langley Field, Va. L-177